Catalysis Today 142 (2009) 138–142

Contents lists available at ScienceDirect

Catalysis Today

journal homepage: www.elsevier.com/locate/cattod

Similarity and differences in the oxidative dehydrogenation of C_2–C_4 alkanes over nano-sized VO_x species using N_2O and O_2

Olga Ovsitser, Evgenii V. Kondratenko *

Leibniz Institute for Catalysis at the University Rostock, Branch Berlin, Richard-Willstätter-Str. 12, D-12489 Berlin, Germany

ARTICLE INFO

Article history:
Available online 31 October 2008

Keywords:
Oxidative dehydrogenation
C_2–C_4 alkanes
Supported VO_x
Nitrous oxide
Oxygen species
TAP reactor
SSITKA

ABSTRACT

The effect of O_2 and N_2O on alkane reactivity and olefin selectivity in the oxidative dehydrogenation of ethane, propane, n-butane, and iso-butane over highly dispersed VO_x species (0.79 V/nm^2) supported on MCM-41 has been systematically investigated. For all the reactions studied, olefin selectivity was significantly improved upon replacing O_2 with N_2O. This is due to suppressing CO_x formation in the presence of N_2O. The most significant improving effect of N_2O was observed for iso-butane dehydrogenation: S(iso-butene) was ca. 67% at X(iso-butane) of 25%.

Possible origins of the superior performance of N_2O were derived from transient experiments using $^{18}O_2$ traces. $^{18}O^{16}O$ species were detected in $^{18}O_2$ and $^{18}O_2$–C_3H_8 transient experiments indicating reversible oxygen chemisorption. In the presence of alkanes, the isotopic heteroexchange of O_2 strongly increased. Based on the distribution of labeled oxygen in CO_x and in O_2 as well as on the increased CO_x formation in sequential O_2–C_3H_8 experiments, it is suggested that non-lattice oxygen species (possibly of a bi-atomic nature) originating from O_2 are non-selective ones and responsible for CO_x formation. These species are not formed from N_2O.

1. Introduction

Oxidative conversion of light alkanes to respective olefins and oxygenates is still a challenging approach in modern oxidation catalysis not only from a fundamental but also from an applied point of view [1–6]. The main challenge is to minimize the formation of carbon oxides (CO_x) in favor of selective products. Selectivity to olefins is significantly increased, and CO_x formation is suppressed, when N_2O is used as oxidizing agent [7–12]. Understanding the origins of the superior performance of N_2O as compared to O_2 may help to identify selective and non-selective pathways/oxygen species. This knowledge is of high scientific and industrial interest to design catalytic materials or catalytic processes performing selectively with O_2, too.

The present contribution was aimed to elucidate the effect of O_2 and N_2O on catalytic performance of highly dispersed surface VO_x species supported over MCM-41 in the oxidative dehydrogenation (ODH) of ethane, propane, n-butane, and iso-butane. To this end, steady-state catalytic tests at different contact times were combined with transient isotopic experiments in vacuum and at ambient pressure using the TAP (temporal analysis of products) and SSITKA (steady-state transient kinetic analysis) reactor systems, respectively. The catalyst has been previously well characterized [10] by various physico-chemical methods (BET, EPR, XRD, *in situ* UV/vis-DRS and Raman spectroscopies as well as H_2-TPR). VO_x species over MCM-41 with vanadium loading up to 5.3 wt.% has been classified as mainly monomer and small two-dimensional VO_x aggregates.

2. Experimental

2.1. Preparation of catalytic materials

VO_x/MCM-41 was prepared by impregnation of MCM-41 with a predetermined amount of vanadium acetyl acetate ($[CH_3COCH{=}C(O-)CH_3]_2VO$) in toluene. The resulting catalyst precursor was calcined at 823 K for 12 h in air. Details of catalyst preparation and characterization have been reported previously [10]. In the present study, a sample with V loading of 5.3 wt.%, designated as VO_x(5)/MCM-41, was used.

2.2. Steady-state catalytic testing

Catalytic measurements were carried out in a U-type fixed-bed reactor made of quartz (i.d. = 6 mm) at T = 773 K and ambient pressure. The catalyst particle size was between 255 and 350 μm.

* Corresponding author. Tel.: +49 30 63924448.
E-mail address: evgenii.kondratenko@catalysis.de (E.V. Kondratenko).

0920-5861/$ – see front matter © 2008 Elsevier B.V. All rights reserved.
doi:10.1016/j.cattod.2008.09.012

The following reaction feeds were used: C_nH_{2n+2}:O_2:Ne = 40:20:40 and C_nH_{2n+2}:N_2O:Ne = 40:40:20, where C_nH_{2n+2} were ethane, propane, n-butane and iso-butane. Ne was used as internal standard for gas chromatographic product analysis (HP-5890 equipped with Poraplot Q and Molsiev 5 columns).

2.3. Transient catalytic experiments

The TAP-2 reactor system has been comprehensively described elsewhere [13]. The catalyst (ca. 20 mg, sieve fraction 250–350 μm) was packed in the micro-reactor made of quartz (40 mm length and 6 mm i.d.) between two layers of quartz of the same particle size. The catalyst was treated in a flow of O_2 (30 ml/min) at 773 K and ambient pressure for ca. 1 h before each experiment. Then, the micro-reactor was evacuated at 773 K to 10^{-5} Pa. Two types of transient experiments were carried out using a pulse size of ca. 10^{15} molecules:

- Single pulsing of C_3H_8:Ne = 1:1 or $^{18}O_2$:Ne = 1:1 over $V^{16}O_x$/MCM-41.
- $^{16}O_2$:Xe = 1:1 and C_3H_8:Ne = 1:1 reaction mixtures were sequentially pulsed over $V^{16}O_x$/MCM-41 from two pulse valves with a time delay of 0.1 s.

Under conditions applied, gas-phase interactions are strongly minimized. Therefore, only heterogeneous reaction steps were under investigation. In the experiments, Ne (99.995%), Xe (99.99%), O_2 (99.995%), and C_3H_8 (99.95%) were used. The $^{18}O_2$ oxygen isotope was purchased from ISOTEC. Transient responses were monitored using a quadruple mass spectrometer (HAL RC 301 Hiden Analytical). For more detailed description see [12].

Steady-state isotopic transient kinetic analysis (SSITKA) experiments were performed in a tubular quartz reactor at 773 K and ambient pressure. Catalyst amount and gas flows were fixed to 80 mg and 30 ml/min (STP), respectively. The following reaction feeds were used: $^{16}O_2$:Ar = 2:98, $^{18}O_2$:Ne:Ar = 2:2:96, C_3H_8:$^{16}O_2$:Ar = 4:2:94 and C_3H_8:$^{18}O_2$:Ne:Ar = 4:2:2:92. Oxygen tracing experiments were performed by switching from non-labeled to labeled reaction feeds after a steady-state operation was achieved with the non-labeled feed. The gas composition at the reactor outlet was monitored by on-line mass spectrometry (Balzer Omnistar). For more experimental details see [14].

3. Results and discussion

3.1. Steady-state performance of oxidative dehydrogenation with O_2 and N_2O

Corresponding olefins, CO and CO_2 were the main carbon-containing products in the oxidative dehydrogenation (ODH) of ethane, propane, n-butane and iso-butane over VO_x(5)/MCM-41 at 773 K using O_2 and N_2O. Another minor products were acetaldehyde, acrolein, ethane, and propane. However, the overall selectivity to these products was not higher as 10% under reaction conditions applied and alkane conversion below 15%. In order to compare the reactivity of highly dispersed VO_x species for alkane oxidation with O_2 and N_2O, the initial rates of alkane conversion as well as the rates of formation of olefins, CO and CO_2 were determined at low degrees of alkane and oxidant conversion ($X(C_nH_{2n+2}) < 5\%$, $X(O_2/N_2O) < 10\%$). These rates are summarized in Table 1. Since the amount of oxygen atoms in O_2- and N_2O-containing feeds was the same, the activity and selectivity of these oxidants in the ODH reactions can be correctly compared. For both oxidants, the initial rate of alkane conversion follows the order: C_2H_6<C_3H_8<n-C_4H_{10}<iso-C_4H_{10}. It is important to highlight that the same order is also valid for the strength of the weakest C–H bond in these alkanes [15,16]. Considering both experimental facts, it is suggested that the breaking of the weakest C–H bond limits the ODH reaction over highly dispersed VO_x species independent of the oxidant applied. However, the oxidant influences strongly the activity and the selectivity. When N_2O is used instead of O_2, the rates of alkane conversion and alkene formation decrease by factor of 3–8 and 1.6–6, while the rates of CO and CO_2 formation become lower in 6–30 and 15–70 times, respectively. Such a dramatic decrease in the CO_x production clearly distinguishes the low ability of N_2O for non-selective alkane/alkene conversion in favor of the selective olefin production.

Table 1
Initial rates of alkane conversion, alkene, CO, and CO_2 formation in ODH reactions of C_2–C_4 alkanes at 773 K over VO_x(5)/MCM-41. Reaction conditions: C_nH_{2n+2}:O_2:Ne = 40:20:40 and C_nH_{2n+2}:N_2O:Ne = 40:40:20; $X(C_nH_{2n+2}) < 5\%$, $X(O_2/N_2O) < 10\%$.

Alkane	Oxidant	Rate (mmol C_nH_{2n+2} g_{cat}^{-1} min^{-1})			
		C_nH_{2n+2}	C_nH_{2n}	CO*	CO_2*
C_2H_6	O_2	0.85	0.16	0.05	0.57
	N_2O	0.15	0.10	0.04	0.006
C_3H_8	O_2	1.5	1.03	0.15	0.31
	N_2O	0.39	0.34	0.025	0.021
n-C_4H_{10}	O_2	3.1	1.7	0.37	0.39
	N_2O	0.45	0.34	0.02	0.028
iso-C_4H_{10}	O_2	4.3	2.6	0.48	0.96
	N_2O	0.56	0.45	0.035	0.041

* The rate of alkane conversion to CO or CO_2 was calculated as mmol of alkane, converted to CO or CO_2.

In order to further elucidate the role of oxidizing agent, ODH catalytic tests were performed at different degrees of alkane conversion. The results obtained are presented in Fig. 1. Irrespective of the oxidant applied, olefin selectivity decreases with an increase in the alkane conversion, while CO_x selectivity increases (data are not shown for brevity). For an O_2-containig feed, primary (extrapolated to zero alkane conversion) alkene selectivity in the ODH of propane, n-butane, and iso-butane is close to ca. 70–80%, while it is only ca. 30% for the ethane ODH. This indicates that direct ethane oxidation to CO_x strongly contributes to the overall CO_x production as compared to the ODH of other alkanes. Upon replacing O_2 with N_2O, olefin selectivity significantly increases (Fig. 1(b)), while CO_x selectivity decreases. The highest effect of N_2O on olefin selectivity was found for the ODH of iso-C_4H_{10}. Primary iso-C_4H_8 selectivity with O_2 is ca. 70–75%, but falls to 10% with an increase in the conversion of iso-C_4H_{10} up to 10%, while CO_x selectivity strongly increases. Such a low ODH performance agrees well with the literature data reporting maximal yield of iso-C_4H_8 of 6–11% [17–21]. The overall CO and CO_2 selectivity was lower than 7% at X(iso-C_4H_{10}) of 25%, when N_2O was used as oxidant. The selectivity towards iso-C_4H_8 amounted to 65% resulting in a yield of 16%.

Irrespective of the alkane applied, two important improving effects of N_2O have been identified for the oxidative dehydrogenation of ethane, propane, n-butane and iso-butane: (i) higher primary olefin selectivity, and (ii) lower decrease in olefin selectivity with increasing alkane conversion, i.e. lower ability for consecutive alkene overoxidation. These results are in agreement with our previous studies of the oxidative dehydrogenation of propane [10]. For deriving deeper insights into primary and secondary reaction pathways of the ODH reaction with O_2 and N_2O over VO_x(5)/MCM-41, transient experiments were carried out in the TAP and SSITKA reactor systems using $^{18}O_2$ traces. Particular attention was paid to CO_x formation and, hence, to the factors

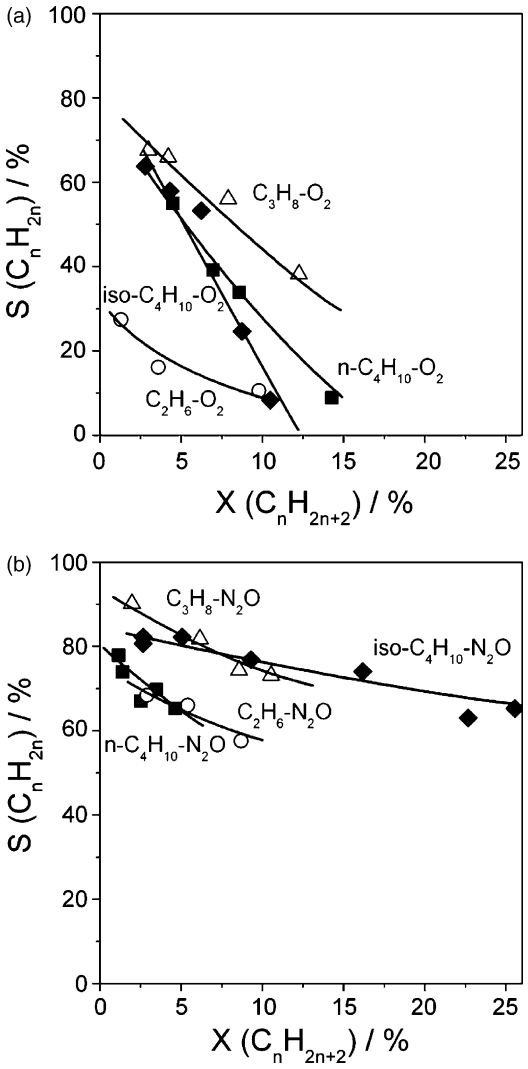

Fig. 1. Selectivity to ethylene (○), propene (△), n-butene (■), and iso-butene (◆) over VO_x(5)/MCM-41 versus alkane conversion using C_nH_{2n+2}:O_2:Ne = 40:20:40 (a) and C_nH_{2n+2}:N_2O:Ne = 40:40:20 (b) mixtures. Conditions: T = 773 K, and P = 1 bar.

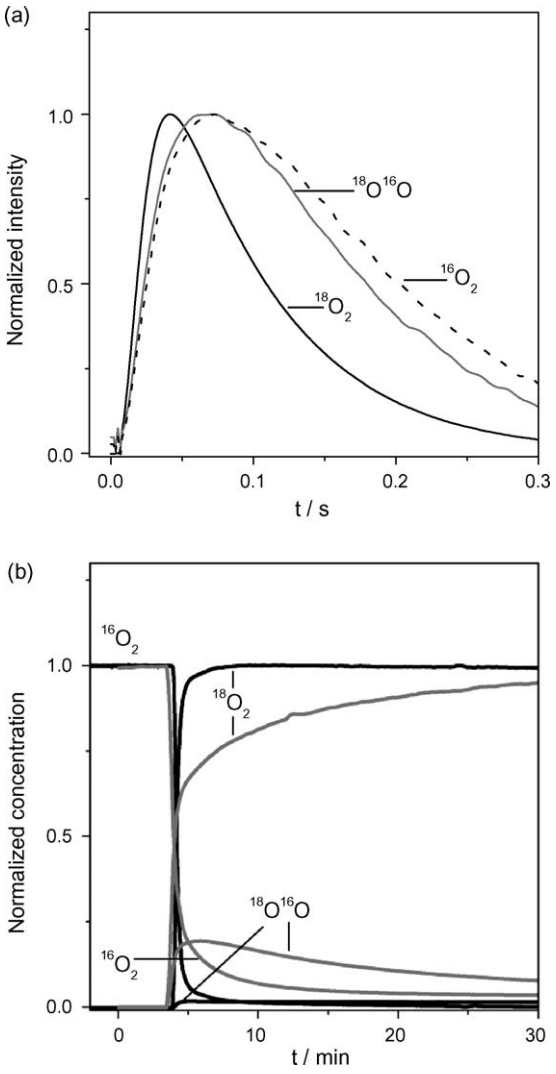

Fig. 2. Oxygen transient responses: (a) upon $^{18}O_2$ pulsing over $V^{16}O_x$(5)/MCM-41 at 823 K in the TAP-reactor; and (b) upon switching from $^{16}O_2$:Ar:Ne = 2:98 to $^{18}O_2$:Ar:Ne = 2:96:2 (black lines) and from C_3H_8:$^{16}O_2$:Ar = 4:2:94 to C_3H_8:$^{18}O_2$:Ar:Ne = 4:2:92:2 (grey lines) at 773 K in the SSITKA reactor system.

determining the olefin selectivity loss. The results are presented below.

3.2. Mechanistic analysis of the ODH reaction with O_2 and N_2O

3.2.1. Interaction of O_2 and N_2O with oxidized and reduced VO_x species

Fig. 2(a) illustrates height-normalized transient responses of $^{18}O_2$, $^{18}O^{16}O$ and $^{16}O_2$ upon pulsing $^{18}O_2$ in the TAP reactor over oxidized $V^{16}O_x$/MCM-41. The normalization was done for better comparing the shape and the order of appearance of gas-phase components. The transient of $^{18}O_2$ appears after the shortest time interval followed by those of $^{18}O^{16}O$ and $^{16}O_2$. The appearance of $^{18}O^{16}O$ before $^{16}O_2$ in the gas-phase indicates simple hetero-exchange mechanism with participation of one lattice oxygen of VO_x species [22]. The formation of $^{18}O^{16}O$ due to homoexchange, i.e. $^{18}O_{2(gas)} + {}^{16}O_{2(gas)} \leftrightarrow {}^{18}O^{16}O_{(gas)}$ [23], can be excluded because $^{16}O_2$ and $^{18}O_2$ were not pulsed together. The presence of $^{18}O^{16}O$ indicates reversible oxygen adsorption over VO_x species. We would like to emphasize that no gas-phase $^{18}O^{16}O$ was detected under similar conditions in our previous work over VO_x/γ-Al_2O_3 in the TAP-reactor [24] and in the literature over VO_x/ZrO_2 [25]. This can be explained by faster incorporation of gas-phase oxygen into VO_x species over VO_x/γ-Al_2O_3 and VO_x/ZrO_2 as compared to VO_x(5)/MCM-41.

The presence of $^{18}O^{16}O$ over VO_x(5)/MCM-41 was also observed at ambient pressure during SSITKA experiments. The transients of oxygen isotopes upon switching from $^{16}O_2$:Ar = 2:98 to $^{18}O_2$:Ar:Ne = 2:96:2 are shown in Fig. 2(b) as black lines. The concentration of non-labeled oxygen ($^{16}O_2$) decreases, while the concentration of labeled oxygen ($^{18}O_2$) increases. The $^{18}O^{16}O$ transient passes over a maximum at ca. 2 min after switching. The presence of $^{18}O^{16}O$ proves that oxidized $V^{16}O_x$ species are active for oxygen isotopic exchange. This means that the double bond in the O_2 molecule is broken and restored, i.e., lattice oxygen of VO_x species is able to activate gas-phase O_2. However, the distribution of oxygen isotopic labels changes, when propane and oxygen are fed together (Fig. 2(b) grey lines). A significantly higher ratio of $^{18}O^{16}O/^{18}O_2$ was detected in the presence of propane. This means that isotopic scrambling is enhanced when propane is present. This difference can be explained by higher concentration of reduced VO_x sites in presence of propane, over which gas-phase oxygen is initially activated and further participates in the oxygen isotopic exchange and in the ODH reaction.

In order to prove whether oxidized VO_x species are active for direct N_2O decomposition, this reaction was studied at 773 K by feeding an N_2O-containing mixture (N_2O:Ne = 40:60) over the catalyst. Only traces of N_2 but no O_2 were detected at the reactor outlet. This means that oxidized VO_x species do not decompose N_2O (reduced VO_x species, which can be formed at 773 K in an O_2-free atmosphere, participate in N_2O decomposition without O_2 formation). We repeated the above experiment, however, in the presence of alkanes. N_2O conversion strongly increases when N_2O and alkane were fed together to the reactor (Table 2). It should be especially emphasized that no gas-phase O_2 was also observed in the experiments with alkane–N_2O mixtures at various conversions of alkane and N_2O. This result can be explained as follows. Alkanes react with oxidized VO_x species yielding reduced ones. The reduced VO_x species are reoxidized by N_2O resulting in gas-phase N_2 and restoring lattice oxygen species. The high activity of reduced VO_x species for N_2O decomposition agrees well with recent DFT calculations of interaction of N_2O with oxidized and reduced isolated and dimeric VO_x species over SiO_2 [26]. Thus, oxidized VO_x species are able to activate O_2 but not N_2O. In the presence of propane, oxidized VO_x species are transformed to the reduced ones, which are highly active for O_2 activation and N_2O decomposition.

3.2.2. Products of propane reactions with VO_x species in the absence and presence of gas-phase O_2

The interaction of C_3H_8 with VO_x(5)/MCM-41 was studied at 773 K by means of single C_3H_8 as well as sequential O_2 and C_3H_8 pulse experiments in the TAP-reactor. In these both experiments, the degree of C_3H_8 conversion did not exceed 2%. In the oxygen-free experiments, C_3H_6 was the only carbon-containing reaction product. Since gas-phase O_2 was not present in the C_3H_8 pulse, it is concluded that C_3H_6 is formed by C_3H_8 oxidation with lattice oxygen of VO_x species. Low amounts of CO and CO_2 could not be unambiguously identified due to overlapping mass spectra of C_3H_8, CO_2, and CO. However, CO_2 was observed, when O_2 and C_3H_8 were sequentially pulsed with a time delay of 0.1 s between the O_2 and C_3H_8 pulses (Fig. 3(a)). A definitive detection of CO was not possible. This result implies that CO_2 formation is accelerated in the presence of gas-phase O_2. Either this could be due to higher oxidation degree of VO_x species when compared to single C_3H_8 pulse experiments in the absence of O_2 or due to the presence of other surface oxygen species, which are formed from gas-phase O_2.

Mechanistic insights into the participation of oxygen from VO_x species and from gas-phase O_2 in CO_2 formation were derived from the analysis of temporal profiles of $C^{16}O_2$, $C^{18}O^{16}O$, and $C^{18}O_2$ formed over $V^{16}O_x$(5)/MCM-41 at 773 K upon switching from a C_3H_8:$^{16}O_2$:Ar = 4:2:94 mixture to a C_3H_8:$^{18}O_2$:Ar:Ne = 4:2:92:2 mixture in the SSITKA set-up at ambient pressure (Fig. 3(b)). Since non-labeled oxygen ($^{16}O_2$) was not present in the latter feed but $C^{16}O_2$ and $C^{18}O^{16}O$ were observed as reaction products, it is concluded that lattice oxygen of VO_x species participates in carbon dioxide formation.

The question here is whether all oxygen species responsible for the formation of CO_2 are chemically equivalent. To this end, we analyze time-on-stream distribution of differently labeled carbon dioxides in Fig. 3(b). The $C^{16}O_2$ transient response approaches zero after ca. 20 min on stream in the C_3H_8:$^{18}O_2$:Ar:Ne = 4:2:92:2 mixture. $C^{18}O^{16}O$ and $C^{18}O_2$, which contain oxygen atoms from gas-phase $^{18}O_2$, start to be formed immediately after switching from a C_3H_8:$^{16}O_2$:Ar = 4:2:94 mixture to a C_3H_8:$^{18}O_2$:Ar:Ne = 4:2:92:2 mixture. However, their transients differ strongly in the shape. The intensity of $C^{18}O^{16}O$ transient increases strongly with time approaching a maximum after ca. 5 min on stream in the C_3H_8:$^{18}O_2$:Ar:Ne = 4:2:92:2 flow followed by a slow decay, while the intensity of the $C^{18}O_2$ transient increases slower, but continuously. The permanent increase of $C^{18}O_2$ production is attributed to slow replacing of non-labeled (^{16}O) lattice oxygen in VO_x species by labeled (^{18}O) ones originating from gas-phase $^{18}O_2$. Another important observation is the difference in the temporal profiles of $C^{16}O_2$ and $C^{16}O^{18}O$ in Fig. 3 (b). These two isotopically labeled carbon dioxides contain ^{16}O, which originates from the lattice oxygen of VO_x species. While the concentration of $C^{16}O_2$ drops to zero within first 20 min on stream in the C_3H_8:$^{18}O_2$:Ar:Ne = 4:2:92:2 flow, the concentration of $C^{16}O^{18}O$ is much higher and similar to $C^{18}O_2$. Let us compare the

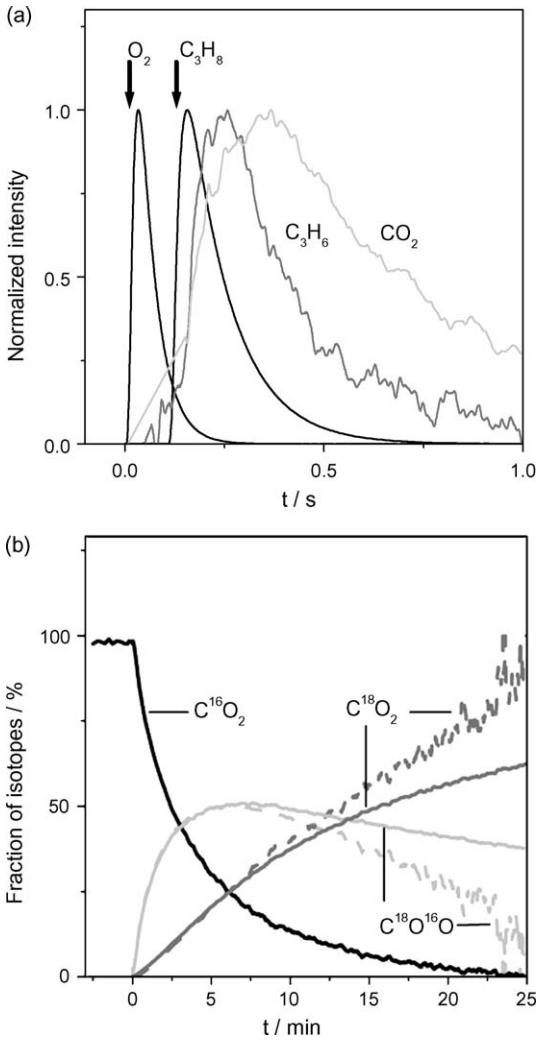

Fig. 3. (a) Transient responses detected in the TAP-reactor during sequential pulsing of O_2 and C_3H_8 (pulse size of C_3H_8 ~5×10^{14} molecules) with a time delay of 0.1 s; (b) fractions of differently labeled carbon dioxides detected in the SSITKA reactor system upon switching from C_3H_8:$^{16}O_2$:Ar = 4:2:94 to C_3H_8:$^{18}O_2$:Ar:Ne = 4:2:92:2. The dashes lines are the results of a statistical simulation as described in the text.

Table 2
N_2O conversion over VO_x(5)/MCM-41 at 773 K in the absence and in the presence of C_2–C_4 alkanes. W/F = 0.1 g·ml^{-1} s.

Reaction mixture (vol%)	X (alkane)/%	X (N_2O)/%
N_2O/Ne = 40/60		0.1
N_2O/C_2H_6/Ne = 40/40/20	1.5	3
N_2O/C_3H_8/Ne = 40/40/20	3.5	9
N_2O/n-C_4H_{10}/Ne = 40/40/20	3.7	11
N_2O/iso-C_4H_{10}/Ne = 40/40/20	4.5	12

above experimental results with a statistical distribution of isotopically labeled oxygen in CO_2 assuming all active surface oxygen species are chemically equivalent. If we express the fraction of ^{18}O in lattice oxygen as y, the fraction of ^{16}O is $(1-y)$. The probability to find two ^{18}O and two ^{16}O atoms in VO_x species is equal to y^2 and $(1-y)^2$, respectively. The probability to find one ^{18}O and one ^{16}O is $2y(1-y)$. From experimentally obtained fraction of $C^{16}O_2$, y can be calculated without any assumption about the kinetics of isotopic exchange. The calculated fractions of differently labeled carbon dioxides are presented in Fig. 3(b) as dotted lines. It has to be repeated that these isotopic distribution should be observed if all the surface oxygen species would be chemically equivalent. It is obvious that the statistical model does not correctly describe the experiment. Therefore, it is suggested that surface oxygen species participating in the formation of CO_2 are not chemically equivalent. However, no definitive conclusion on the nature of these oxygen species could be derived from our experiments. Recent DFT calculations of interaction of O_2 and N_2O with reduced and oxidized VO_x species suggest that peroxo species are formed upon interaction of O_2 but not N_2O with reduced VO_x species [26]. These bi-atomic oxygen species are further transformed to lattice oxygen ones. The latter species are also formed upon reoxidation of reduced VO_x species by N_2O. Our transient results in Section 3.2 in agreement with literature demonstrate that lattice oxygen participates in both selective alkane dehydrogenation and non-selective CO_x formation. According to the DFT calculations in [26], peroxovanadates, which are formed from O_2 only, are highly reactive for consecutive propene oxidation to CO_x. At this stage, it is important to stress that the slope of the ODH selectivity-conversion relationships in Fig. 1 depends on the oxidant applied. This slope reflects the catalyst ability for consecutive combustion of primarily formed olefins to CO_x. Upon replacing O_2 with N_2O, olefin selectivity in the ODH decreases slower with an increase in alkane conversion indicating lower ability of N_2O for consecutive olefin oxidation. This experimental result nicely correlates with the theoretical predictions. It is also important to mention the following order of consecutive olefin oxidation with O_2: $C_2H_4 \leq C_3H_6 < n\text{-}C_4H_8 \leq iso\text{-}C_4H_8$. This order is also valid for the stability of ions or radicals formed from the respective alkanes by abstraction of one hydrogen atom. Based on these experimental facts it can be suggested that the long-living ions/radicals are easily oxidized to CO_x.

Based on the above experimental results and DFT calculation in [26], the improving effect of N_2O on the ODH selectivity over highly dispersed VO_x species supported over MCM-41 can be due to the inability of N_2O to generate non-selective oxygen species originating upon reoxidation of reduced VO_x species by O_2. However, there is a need for direct experimental evidences. Our experimental effort to unravel the nature of these oxygen species is now in progress.

4. Summary

The oxidative dehydrogenation of ethane, propane, n-butane and iso-butane to respective olefins with O_2 and N_2O was investigated over highly dispersed VO_x species supported over MCM-41. Irrespective of the alkane and the oxidant applied, the overall rate of alkane conversion increases with a decrease in the strength of the weakest C–H bond in the alkane molecule indicating that alkane activation is the rate-limiting step. Upon replacing O_2 with N_2O, the overall activity decreases but the olefin selectivity increases. The selectivity increase is due to suppressing non-selective production of CO and CO_2 via direct alkane combustion and consecutive alkene oxidation.

Transient experiments in the TAP reactor and in a SSITKA set up evidenced, that N_2O does not decompose over oxidized VO_x species in the absence of alkane, while heterogenenous oxygen isotopic exchange between gas-phase $^{18}O_2$ and lattice ^{16}O of VO_x species takes place yielding $^{18}O^{16}O$. The presence of mixed oxygen isotope proves reversible dissociative O_2 adsorption over oxidized VO_x species. Both, the decomposition of N_2O and the oxygen isotopic exchange are significantly accelerated in the presence of alkanes indicating that reduced VO_x species are more reactive for these processes than the oxidized ones.

TAP results, and SSITKA data consistent with Mar-van-Krevelen mechanism, where selective, and non-selective reactions occur on lattice oxygen of VO_x species. This is valid for O_2- and N_2O-containing feeds. O_2 and C_3H_8 sequential pulsing in the TAP reactor and $^{16}O_2$–C_3H_8/$^{18}O_2$–C_3H_8 SSITKA experiment indicate that CO_x formation in the presence of O_2 involves additional another type of oxygen species. These oxygen species are assumed to be of molecular nature and are not formed from N_2O. This may be a reason of the superior performance of N_2O over O_2.

Acknowledgements

Support by Deutsche Forschungsgemeinschaft (DFG) within the collaborative research center (Sonderforschungsbereich) 546 "Structure, dynamics and reactivity of transition metal oxide aggregates" has been greatly appreciated. The authors also thank Dr. R. Fortrie for a statistical simulation of SSITKA results.

References

[1] E.A. Mamedov, V.C. Cortes, Corberan, Appl. Catal. A 127 (1995) 1.
[2] M. Baerns, O. Buyevskaya, Catal. Today 45 (1998) 13.
[3] M.A. Banares, Catal. Today 51 (1999) 319.
[4] W. Ueda, N.F. Chen, K. Oshihara, Kinet. Catal. 40 (1999) 447.
[5] F. Cavani, F. Trifiro, Catal. Today 36 (1997) 431.
[6] J.M. Lopez Nieto, Topic Catal. 41 (2006) 3.
[7] E.V. Kondratenko, M. Baerns, Appl. Catal. A 222 (2001) 133.
[8] J. Pérez-Ramírez, E.V. Kondratenko, Chem. Commun. (2003) 2152.
[9] F. Dury, M.A. Centeno, E.M. Gaigneaux, P. Ruiz, Catal. Today 81 (2003) 95.
[10] E.V. Kondratenko, M. Cherian, M. Baerns, X. Su, R. Schlögl, X. Wang, I.E. Wachs, J. Catal. 234 (2005) 131.
[11] R. Bulánek, B. Wichterlová, K. Novoveská, V. Kreibich, Appl. Catal. A 264 (2004) 13.
[12] O. Ovsitser, M. Cherian, E.V. Kondratenko, J. Phys. Chem. C 111 (2007) 8594.
[13] J.T. Gleaves, G.S. Yablonsky, P. Phanawadee, Y. Schuurman, Appl. Catal. A 160 (1997) 55.
[14] E.V. Kondratenko, O. Ovsitser, J. Radnik, M. Schneider, R. Kraehnert, U. Dingerdissen, Appl. Catal. A 319 (2007) 98.
[15] J.A.M. Simoes, J.L. Beauchamp, Chem. Rev. 90 (1990) 629.
[16] S.L. Khursan, React. Kinet. Catal. Lett. 51 (1993) 95.
[17] G. Neri, A. Pistone, S. De Rossi, E. Rombi, C. Milone, S. Galvagno, Appl. Catal. A. 260 (2004) 75.
[18] B.Y. Jibril, N.O. Elbashir, S.M. Al-Zahrani, A.E. Abasaeed, Chem. Eng. Proc. 44 (2005) 835.
[19] B. Grzybowska, J. Sloczynski, R. Grabowski, K. Wcislo, A. Kozlowska, J. Stoch, J. Zielinski, J. Catal. 178 (1998) 687.
[20] V. Cortés Corberán, M.J. Jia, J. El-Haskouri, R.X. Valenzuela, D. Beltrán-Porter, P. Amorós, Catal. Today 91–92 (2004) 127.
[21] F. Cavani, R. Mezzogori, A. Trovarelli, J. Mol. Catal. A 204–205 (2003) 599.
[22] C. Descorme, Y. Madier, D. Duprez, J. Catal. 196 (2000) 167.
[23] G. Boreskov, Adv. Catal. 15 (1964) 285.
[24] E.V. Kondratenko, N. Steinfeldt, M. Baerns, PCCP 8 (2006) 1624.
[25] K. Chen, A. Khodakov, J. Yang, A.T. Bell, I. Iglesia, J. Catal. 186 (1999) 325.
[26] X. Rozanska, E.V. Kondratenko, J. Sauer, J. Catal. 256 (2008) 84.